Effect of a Complex Formation on the Calculated Low-Pressure Rate Constant of a Bimolecular Gas-Phase Reaction Governed by Tunneling

LAURA MASGRAU, ÀNGELS GONZÁLEZ-LAFONT, JOSÉ M. LLUCH

Departament de Química, Universitat Autònoma de Barcelona, 08193 Bellaterra, Barcelona, Spain

Received 16 April 1999; accepted 12 July 1999

ABSTRACT: Many important bimolecular hydrogen-transfer processes that take place in the atmosphere proceed via a potential energy minimum (hydrogen-bonded complex) that precedes along the minimum energy path the unique saddle point of the reaction, the one corresponding to the hydrogen transfer. It is clear that the one-step low-pressure rate constant of such a reaction does not depend on the existence of any complex along the minimum energy path below the reactant if the reaction takes place by thermal activation over a transition state that lies quite above the reactants (for instance 10 kcal/mol). However, we have quantitatively shown in this article that the scenario notoriously changes if the reaction involves significant tunneling. In this work, we have theoretically calculated the rate constants and their temperature dependence for the reaction HO + HOH → HOH + OH by means of a canonical variational transition state theory and a canonical unified statistical theory (when necessary). Multidimensional tunneling effects have been included with a semiclassical transmission coefficient. Two kinds of modified potential energy surfaces (PESs), obtained from an original *ab initio* potential energy surface, previously calculated by us, have been used. The Eckart-modified PESs serve to model the hydrogen-abstraction profiles with no complexes along the path, while the Gaussian-modified PESs model the energy profiles with two complexes along the path symmetrically distributed at each side of the abstraction saddle point. Our results show that the existence of those complexes reduces the thickness of the classically forbidden region for energies below the adiabatic barrier, and then tunneling is promoted and the reaction is accelerated. The effect of the complex formation in several kinetic magnitudes, as the Arrhenius parameters and the kinetic isotope effect has also been analyzed.
J Comput Chem 20: 1685–1692, 1999

Keywords: low-pressure rate constant; hydrogen-bonded complex; tunneling; modified potential energy surfaces; Arrhenius parameters

Correspondence to: J. M. Lluch; email: lluch@klingon.uab.es
Contract/grant sponsor: Dirección General de Enseñanza Superior (DGES); contract/grant number: PB95-0637

CCC 0192-8651 / 99 / 201685-08

Introduction

Atmospheric chemistry has received a great deal of attention in the recent years.[1] Progress in this field has been made it possible due to the improvement of both the experimental techniques and the theoretical methods that are employed to determine the rate constants of the reactions that take place in the Earth's atmosphere. A particularly interesting class of reactions are those bimolecular gas-phase processes that proceed via a potential energy minimum that precedes along the minimum energy path: the unique saddle point of the reaction. Normally, that minimum is a hydrogen-bonded complex that forms monotonically downhill from the reactants without a classical potential energy barrier.[2] In this case, dynamical considerations imply that the complex is initially formed in highly excited rovibrational states, very far from the thermal equilibrium situation in which the ground vibrational state is the most populated. Then, depending on the experimental conditions, two different reaction mechanisms are possible.[3] Under high-pressure conditions, as a result of many collisions with other molecules, the complex will eventually lose its excess energy and reach a thermal distribution. The global reaction will take place through an indirect mechanism involving two consecutive steps: the formation of a thermalized intermediate followed by the reaction of that intermediate itself, the two kinetic steps being independent. Conversely, for the low-pressure limit of the reaction, where bimolecular complexes are not perturbed by collisions with third bodies, the energy relaxation process does not occur, and the global reaction proceeds from reactants to products in a single kinetic step.

Let us focus now on the low-pressure regime. Despite the existence of the potential energy minimum, no intermediate is stabilized. Then, does that minimum play any kinetic role? To answer this question one has to realize that the appearance of the complex in terms of potential energy leads to two dynamical bottlenecks along the reaction path in terms of generalized free energy of activation: one in the association region (from the reactants to the complex), and the other in the region around the saddle point. According to the canonical unified statistical theory (CUS),[4] the reaction rate constant $k(T)$ of the unique kinetic step is given by

$$\frac{1}{k(T)} = \frac{1}{k_{as}(T)} - \frac{1}{k_C(T)} + \frac{1}{k_{sp}(T)} \qquad (1)$$

where k_{as} and k_{sp} are, respectively, the rate constants for passage through those two bottleneck regions and k_C denotes the one-way flux rate constant evaluated at the complex. Usually,[2c, 5] the saddle point potential energy lies quite above both the reactants and the complex, in such a way that k_{as} and k_C turn out to be very big in comparison with k_{sp} at the normal range of temperatures of these reactions. So, the rate constant $k(T)$ of eq. (1) is reduced to $k_{sp}(T)$, formally as though the complex (and, therefore, the association bottleneck) does not exist. Then, at first glance, it would seem that, in these circumstances, the complex does not play any role in the reaction kinetics, and that its existence could be ignored.

The purpose of this article is to show how, if the reaction involves a significant tunneling, the existence of the potential energy minimum corresponding to a complex formation in the minimum energy path is crucial to determine the shape of the potential energy surface in such a way that it plays a key role in the one-step low-pressure rate constant $k(T)$ and other measurable kinetic magnitudes as the Arrhenius parameters and the kinetic isotope effects. Our conclusions will be applicable to a wide range of reactions, because many of the atmospheric reactions that proceed first forming a hydrogen-bonded complex involve later a hydrogen-transfer process for which tunneling can be expected.

Method of Calculation

To quantitatively describe how the existence of a potential energy minimum corresponding to a complex on the minimum energy path may influence the low-pressure rate constant $k(T)$ of an atmospheric reaction in which tunneling is important, we have carried out in this work a series of model calculations based on the gas-phase radical-molecule identity reaction HO+HOH → HOH+OH, already studied by us in a previous article.[2c] In the present work we have performed additional kinetic calculations on that process in which we modified the shape of the potential energy hypersurface (PES).

At this point, and to understand the methodology we have employed in the present study, some details of the previous work have to be recapitulated. The classical energy profile for the HO + HOH → HOH + OH reaction as a function of s, where s denotes the distance along the reaction path in an isoinertial mass-weighted coordinate system, is depicted in Figure 1. The reaction path was calculated at the UMP2/6-311G(3d,2p) level with single-point energy corrections at the CCSD(T)/6-311G(3d,2p) level performed all along the path (see

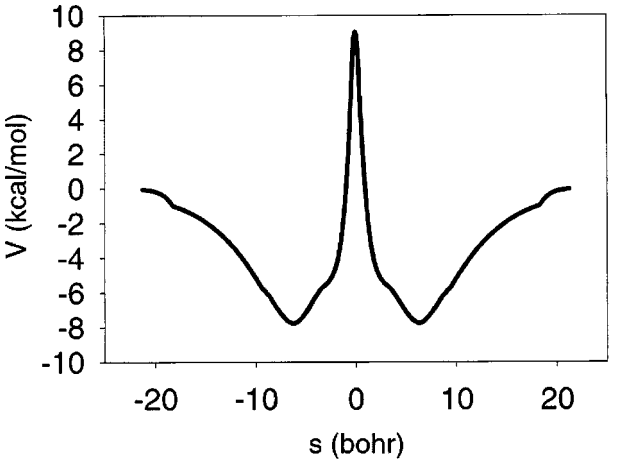

FIGURE 1. Classical energy curve ($V_{RP,M}$) with respect to the reactants separated at infinite distance as a function of s along the MEP connecting the C and C′ complexes. The coordinates are scaled to a mass of 1 amu.

ref. 2c for further details). Several regions can be distinguished along the classical energy profile of Figure 1: an association region from the reactants to the hydrogen-bonded reactant complex C, formed as the hydroxyl radical and the water molecule approach each other with no classical energy barrier; an abstraction region from the reactant complex C to the product complex C′, where the hydrogen abstraction itself takes place with a saddle point that represents a positive classical energy barrier with respect to the reactants; and finally, a dissociation region from complex C′ to the products. Note that the reaction path for the perprotio reaction is symmetric. A generalized normal-mode analysis was performed in rectilinear coordinates, and the RODS algorithm[6] was used to improve the generalized frequencies along the path. This allowed us to calculate the vibrationally adiabatic ground-state energy curve as a function of s,

$$V_a^G(s) = V_{RP,M}(s) + \varepsilon_{tran}^G(s) \tag{2}$$

where $V_{RP,M}(s)$ (the classical energy profile of Fig. 1) is the minimum classical energy in the reoriented dividing surface at s on the reaction path and $\varepsilon_{tran}^G(s)$ is the zero-point energy (ZPE) at s from the generalized normal-mode vibrations transverse to the reaction path. This reaction path has been constructed as a distinguished reaction coordinate (by fixing the internuclear distance between the water oxygen atom and the hydrogen atom in the hydroxyl radical at different values and allowing the other degrees of freedom to relax) in the association and dissociation regions and following the minimum energy path (MEP) in the abstraction region. The $V_a^G(s)$ curve in the abstraction region presents a clear maximum at the saddle point ($s = 0$) with an adiabatic energy barrier V_a^G of 11.72 kcal/mol (for reactants $V_a^G = 0$), whereas neither of the corresponding ground-state adiabatic curves in the association and dissociation regions presents an energetic maximum. So, the $V_a^G(s)$ curve monotonically decreases from reactants to complex C, with an adiabatic depth at this complex, $(V_a^G)_C$, of −5.5 kcal/mol, and this same $V_a^G(s)$ curve monotonically increases from complex C′ up to products.

In the present work, we have performed additional calculations on the process HO + HOH → HOH + OH in which we modified the shape of the original PES, with the purpose of showing, in a quantitative fashion, how the existence of a complex on the path between the reactants and the hydrogen-abstraction transition state can provoke a faster fall of the adiabatic energy moving away from that transition state and, therefore, can reduce the width of the classically forbidden region. On these modified PESs, several key features of the previously calculated *ab initio* PES have not been changed. In particular, the symmetry of the energetic profile has been maintained as well as the classical potential energy barrier height and the vibrationally adiabatic ground-state barrier height for the hydrogen abstraction process (the later is equivalent to the activation free energy at $T = 0$ K). Moreover, the corresponding free-energy barriers associated with the saddle point at higher temperatures turn out to be invariant also.

Two different kinds of modified PESs have been tested. On one hand, and mainly for the sake of comparison, we have modeled a classical potential energy profile with no complex formation by using an analytic Eckart function. This function has the form

$$V(s) = \frac{AY}{1+Y} + \frac{BY}{(1+Y)^2} \tag{3a}$$

$$Y = e^{(s-S_0)/L} \tag{3b}$$

where A, B, and L are independent parameters, and S_0 determines the location of the maximum of V along the s axis. We determine S_0 such that this maximum occurs at $s = 0$ (i.e., at the saddle point). Thus,

$$A = V(s = \infty) \tag{4a}$$

$$B = (2V^{\neq} - A) + 2\left[V^{\neq}(V^{\neq} - A)\right]^{1/2} \tag{4b}$$

$$S_0 = -L \ln\left(\frac{A+B}{B-A}\right) \tag{4c}$$

where $V^{\neq}$ is the classical barrier height. A equals the classical endoergicity since $V(s = -\infty) = 0$ by convention. Notice that for a symmetric Eckart, $S_0 = 0$ and $A = 0$. The range parameter L is obtained using the second-order global interpolation procedure.[7] This model assumes that information is available at reactants, saddle point, products, and two extra points, $s = s_1$ and $s = s_2$, on the reaction path, near the saddle point. In this particular case, the two extra points at $s_1 = -0.032$ bohr and at $s_2 = 0.032$ bohr have been taken from the *ab initio* MEP on the original PES. Within this model, V is modeled by eqs. (3a) and (3b) by taking L as the average between the value obtained by requiring that the Eckart function goes through $s = 0$ and $s = s_1$ and the value obtained by requiring that it goes through $s = 0$ and $s = s_2$. The fitted value finally used for L is 0.38 bohr. The product $I(s)$ of the principal moments of inertia and the adiabatic energy curve $V_a^G(s)$ are also needed to calculate the rate constants. The $I(s)$ function is obtained in accordance with the second-order global interpolation model,[7] whereas the adiabatic curve has been modeled in this work by an Eckart function with no complex formation of the form

$$V_a^G(s) = \frac{ay}{1+y} + \frac{by}{(1+y)^2} + c \tag{5a}$$

$$y = e^{(s-s_0)/l} \tag{5b}$$

where a, b, c, and l are independent parameters, and s_0 determines the location of the maximum of V_a^G along the s axis. In fitting V_a^G, we have

$$a = V_a^G(s = +\infty) - V_a^G(s = -\infty) \tag{6a}$$

$$b = \left(2V_a^{\mathrm{AG}} - a\right) + 2\left[V_a^{\mathrm{AG}}\left(V_a^{\mathrm{AG}} - a\right)\right]^{1/2} \tag{6b}$$

$$c = \varepsilon_{\mathrm{tran}}^G(s = -\infty) \tag{6c}$$

$$s_0 = s_*^{\mathrm{AG}} - l \ln\left(\frac{a+b}{b-a}\right) \tag{6d}$$

where V_a^{AG} denotes the vibrationally adiabatic ground-state barrier height relative to reactants, and s_*^{AG} indicates the location of the adiabatic maximum on the reaction path. In fact, the analytical Eckart function for the classical energy profile [eqs. (3a) and (3b)] was only needed to variationally locate that maximum on the adiabatic curve. Notice that for a symmetric Eckart $a = 0$ and $s_0 = s_*^{\mathrm{AG}}$. As indicated below, no variational effects are obtained for the abstraction process on the modified PESs, in agreement with the results for the original PES. So, $V_a^{\mathrm{AG}} = (V_a^G)^{\neq}$ and $s_*^{\mathrm{AG}} = 0$. Then, we have modeled a series of adiabatic curves of increasing width by augmenting the adiabatic range parameter l from an initial fitted value. The initial value of $l = 0.19$ bohr has been obtained by a four-point fit of the adiabatic Eckart function to the original zero point energies at reactants, at products, at $s = s_*^{\mathrm{AG}}$ and at $s = s_1$. Finally, to calculate the tunneling corrections, we have interpolated the effective mass $\mu(s)$ by an inverted symmetric Eckart function, following the indications of the second-order global interpolation procedure and using the information from the original PES.

The second type of potential energy surfaces modeled in this work contains two minima below the reactants symmetrically distributed at each side of the saddle point of the abstraction process. The analytic function for the modified $V(s)$ is obtained in this case by using the interpolation method based on corrections at three points on the reaction path known as IC, which denotes interpolated corrections.[8] The three points are: the saddle point, and two stationary points—one on the reactant side of the reaction path (complex C in our reaction), and the other one on the product side (complex C′ in our reaction). The modified $V(s)$ is obtained by adding a correction function $\Delta V(s)$ to the original classical potential energy profile (see Fig. 1) from the reactant complex C to the product complex C′. For the correction function $\Delta V(s)$, we use two cutoff Gaussian functions—one for the reactant side, and the other one of the product side of the MEP, of the form

$$\Delta V = A_M \exp\left(-\frac{B_M}{1 - (s/s_{\mathrm{MW}})^2}\right) + C_M \tag{7}$$

where

$$A_M = \left[\Delta V^{\neq} - \Delta V(s = s_{\mathrm{MW}})\right] \exp(B_M) \tag{8a}$$

$$C_M = \Delta V(s = s_{\mathrm{MW}}) \tag{8b}$$

The value of ΔV at $s = 0$ is denoted $\Delta V^{\neq}$ and B_M is the range parameter for reactants ($M = R$) or products ($M = P$). s_{MW} denotes the location of the reactant ($M = R$) or product well ($M = P$). Each cutoff Gaussian correction function is solely determined by the correction at $s = 0$ and either at $s = s_{\mathrm{RW}}$ or $s = s_{\mathrm{PW}}$ with B_R and B_P determined by imposing that the cutoff Gaussian functions go through $s = -1.01$ bohr and $s = 1.01$ bohr [at those two s values, $V(s) = 1/2(V^{\neq} - V_C)$ on the original PES; $V^{\neq}$ stands for the classical energy barrier height, and V_C corresponds to the classical energy depth of the complexes, both energetic magnitudes calculated with respect to reactants]. In our particular application of these correction functions, $\Delta V^{\neq}$ is forced to be zero, because we want to keep the classical abstraction energy barrier invariant on the modified PESs. $\Delta V(s = s_{\mathrm{RW}}$ and $s = s_{\mathrm{PW}})$ have been modified to model potential energy profiles with

different well depths on the path. The product of the principal moments of inertia, $I(s)$, and the frequencies, $\omega_i(s)$, along the path from C to C′ have not been corrected, and the effective reduced mass for tunneling is also calculated using only information from the original calculated PES.

In this article the rate constants have been calculated using the canonical variational transition state theory (CVT)[4a, 9], and including multidimensional quantum effects on the nuclear motion by a transmission coefficient obtained within the small-curvature tunneling (SCT) semiclassical adiabatic ground-state approximation.[10] On the Eckart-modified PESs the HO + HOH → HOH + OH reaction has only one dynamical bottleneck in the region corresponding to the hydrogen abstraction saddle point. This way, the rate constant $k^{CVT/SCT}$ for the hydrogen transfer itself is equivalent to the reaction rate constant $k(T)$. On the Gaussian-modified PESs, because two complexes, C and C′, appear along the reaction path, there are three dynamical bottlenecks in the reaction: (a) in the association region; (b) in the abstraction region; (c) in the dissociation region. According to the canonical unified statistical theory (CUS),[4] the reaction rate constant $k(T)$ is given by

$$\frac{1}{k(T)} = \frac{1}{k_{as}(T)} - \frac{1}{k_C(T)} + \frac{1}{k_{sp}(T)} - \frac{1}{k_{C'}(T)} + \frac{1}{k_{di}(T)} \quad (9)$$

where k_{as}, k_C and k_{sp} have been defined in the introduction section, k_{di} stands for the rate constant for passage through the dissociation bottleneck region, and $k_{C'}$ is the one-way flux rate constant at complex C' [differences between eqs. (9) and (1) arise from the fact that the first one includes the effect of the formation of two complexes]. Due to the significant adiabatic energy barrier in the hydrogen abstraction saddle point region using the Gaussian-modified PESs, the k_{sp} rate constant is clearly lower than the k_C, $k_{C'}$, k_{as}, and k_{di} rate constants, in such a way that the final CUS rate constant $k(T)$ in eq. (9) is reduced to its single important contribution, namely, the k_{sp} rate constant (calculated as a $k^{CVT/SCT}$ rate constant). In agreement with the original PES, the hydrogen abstraction process does not present any variational effect on the modified PESs.

The Arrhenius parameters at different temperatures have also been calculated on the two kinds of modified PESs. Finally, the primary kinetic isotope effect for the reaction HO + DOD → HOD + OD has been evaluated for each one of the Gaussian-modified classical energy profiles in which the reaction path distances were recalculated for the deuterated reaction. The product of the principal moments of inertia, the frequencies, and the reduced mass for tunneling, have been calculated by using the same IC algorithms as in the perprotio reaction but with the value of those magnitudes adequately corrected for the isotope effect.

The Eckart-modified PESs were calculated by using a program developed in our group for the second-order global interpolation model, whereas the version 7.9.1 of the POLYRATE computer program[11] was used for the Gaussian-modified PESs.

Results and Discussion

In this section, for the sake of comparison, we will first present the results corresponding to the potential energy surfaces without a complex formation. Then we will discuss the calculations for the surfaces with two complexes. We note that all the potential energy surfaces are assumed to correspond to the low-pressure gas-phase HO + HOH → HOH + OH reaction, for which tunneling is important.

The adiabatic energy curves displayed in Figure 2 do not involve any complexes formation. For this cases, $V_a^G(s)$ monotonically increases from the reactants ($s = -\infty$) to the transition state ($s = 0$; no variational effect at any temperature), and monotonically decreases from the transition state to the products ($s = \infty$). All the cases involve the same adiabatic energy barrier (11.72 kcal/mol) and identical free-energy barrier as a function of the temperature. For each curve Table I shows the adiabatic range parameter l (which determines the thickness of the Eckart function), the rate constant of

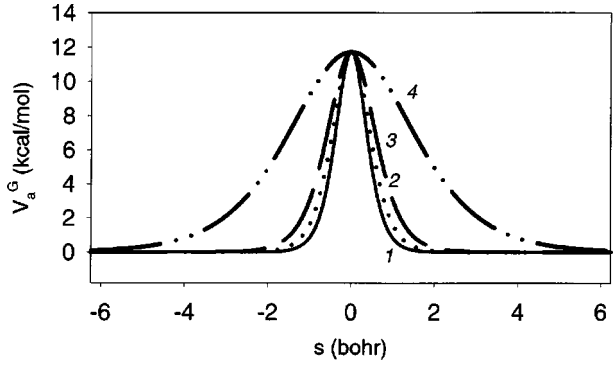

FIGURE 2. Adiabatic energy curves with respect to the reactants separated at infinite distance as a function of s. These curves do not involve any complex formation. The coordinates are scaled to a mass of 1 amu.

TABLE I.

Eckart's Adiabatic Range Parameters (in Bohr), Rate Constants (in cm^3 $Molecule^{-1}$ s^{-1}) at 300 K (Power of 10 in Parentheses), and Transmission Coefficients at 300 K for the Reactions Corresponding to the Four Curves Depicted in Figure 2.

Curve	l	$k^{CVT/SCT}$	κ^{SCT}
1	0.25	7.62(−19)	98.1
2	0.30	1.83(−19)	23.6
3	0.39	5.06(−20)	6.52
4	1.0	9.87(−21)	1.27

the reaction including the SCT tunneling correction ($k^{CVT/SCT}$), and the corresponding SCT transmission coefficient (κ^{SCT}) at 300 K. Because the free-energy barrier height does not vary among curves 1 to 4, according to the transition state theory the rate constant without tunneling correction (k^{CVT}) does not modify either. The differences in $k^{CVT/SCT}$ stem exclusively from the transmission coefficient. κ^{SCT} accounts for the dynamical quantum effects of reaction-coordinate tunneling and nonclassical reflection, and is given by the ratio of thermally averaged quantal transmission probability to the thermally averaged classical transmission probability for the same vibrationally adiabatic barrier. As seen in Figure 2, curve 4 could be a rather reasonable adiabatic profile for a bimolecular reaction, reaching the adiabatic energy of the reactants (and of the products given the symmetry of the reaction) beyond 6 bohr from the transition state. The resulting classical forbidden region for the energies below the adiabatic barrier is quite wide, leading to a transmission coefficient (1.27) that is only slightly larger than unity. If the fall from the transition state is forced (in such a way that the value of the reactants is attained before 2 bohr from the transition state) the curves 3, 2, and 1 are obtained. As expected, it can be seen in Table I that for the narrower curves the transmission coefficient becomes greater as a consequence of the increase of the quantal transmission probabilities, whereas the corresponding classical transmission probabilities remain invariant.

The change in the tunneling contribution to the reaction has a well-known, large effect on the Arrhenius parameters. The preexponential factors and activation energies at 300 K, over the range 300–420 K, and at 700 K for the four curves shown in Figure 2, are presented in Table II. Activation energies are obtained from rate constants through the usual definition

$$E_a = -R\frac{d(\ln k(T))}{d(1/T)} \tag{10}$$

which is equivalent to determining the slope of an Arrhenius plot. Each preexponential factor corresponds to the value at which the straight line tangent to the plot intercepts the $\ln k$ axis at infinite temperature. Note that in absence of tunneling the four curves would lead to the same linear Arrhenius plot (no curvature) with identical activation energies and preexponential factors, independently on the temperature. However, as expected, the slopes of the Arrhenius plots, and therefore, the activation energies, decrease as tunneling becomes more dominant for the narrower adiabatic curves at a given temperature or at lower temperatures for a given curve. Combining these two trends, it can be seen that the hypothetical reactions associated with the wider adiabatic potential energy curves (that is, with a lesser tunneling contribution) approach classical Arrhenius behavior faster as the temperature increases. On the other hand, the variation of the preexponential factors parallels the corresponding variation of the activation energies, because the infinite temperature intercepts change as a consequence of the curvature induced by tunneling.

TABLE II.

Preexponential Factors (in cm^3 $Molecule^{-1}$ s^{-1}) and Activation Energies (in kcal/mol) at Several Temperatures (Power of 10 in Parentheses) for the Reactions Corresponding to the Four Curves Depicted in Figure 2.

	300 K		300–420 K		700 K	
Curve	A	E_a	A	E_a	A	E_a
1	1.60(−15)	4.57	1.35(−14)	5.83	1.06(−12)	10.11
2	6.66(−15)	6.26	4.73(−14)	7.43	1.22(−12)	10.68
3	5.56(−14)	8.29	1.76(−13)	8.99	1.70(−12)	11.35
4	7.41(−13)	10.82	8.37(−13)	10.89	2.06(−12)	11.92

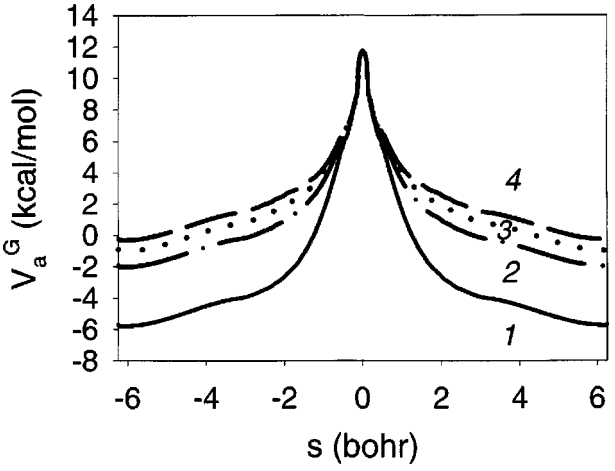

FIGURE 3. Adiabatic energy curves with respect to the reactants separated at infinite distance as a function of *s*. Each curve contains two complexes. The coordinates are scaled to a mass of 1 amu.

Up to now we have artificially reduced the width of the adiabatic energy surface below the barrier, in this way, as expected, modifying the tunneling contribution and provoking large changes in several kinetic parameters. Now we will show that the same effect can be naturally produced if a potential energy minimum appears along the minimum energy path of the reaction. To this aim, all the adiabatic potential energy curves depicted in Figure 3 contain two minima ($s = \pm 6.24$ bohr) below the reactants, symmetrically distributed at each side of the saddle point. These minima force the region with adiabatic energy above the reactants ($V_a^G = 0$) to be confined very close to the transition state. In other words, in absence of such minima, $V_a^G(s)$ begins to increase above the reactants already at long distance from the transition state, forming a very wide energy mountain that is not easy to cross by tunneling. Conversely, as a result of the existence of the minimum, $V_a^G(s)$ monotonically decreases from the reactants to the minimum corresponding to the reactants side, and then grows to reach the transition state (the products side reproduces symmetrically that situation for the present reaction). So the range of values of *s* where $V_a^G > 0$ is narrow, in such a way that the thinness of the classically forbidden region for energies below the adiabatic barrier favors tunneling. As seen in Table III (which refers to adiabatic energy curves depicted in Fig. 3), the larger the depth of the well, the larger the tunneling contribution given by κ^{SCT}, leading to greater values of the $k^{CVT/SCT}$ rate constant. Note that in building up the four curves of Figure 3 we have kept common the region with

TABLE III.
Classical Energies of Complexes (kcal/mol) with Respect to the Reactants, Adiabatic Depth of Complexes (kcal/mol) with Respect to the Reactants, Rate Constants (in cm^3 $Molecule^{-1}$ s^{-1}) at 300 K (Power of 10 in Parentheses), Transmission Coefficients at 300 K, and Kinetic Isotope Effects for the Reactions Corresponding to the Four Curves Depicted in Figure 3.

Curve	V_C	$(V_a^G)_C$	$k^{CVT/SCT}$	κ^{SCT}	KIE (k_H/k_D)
1	−7.8	−5.5	1.82(−17)	2334	25.49
2	−4.0	−1.8	6.72(−18)	865	18.37
3	−3.0	−0.8	5.34(−18)	686	17.20
4	−2.3	−0.1	4.45(−18)	573	16.05

$V_a^G > 6$ kcal/mol. As a matter of fact, even this high-energy region would probably become somewhat wider as the depth of the well diminishes. Ignoring this fact in Figure 3, we have underestimated the loss of tunneling contribution as the minimum progressively disappears, which reinforces our argument on the effect of the complex formation. At this point it should be recalled that the free energy barrier associated with all curves in Figure 3 is the same as for the curves in Figure 2, so that the k^{CVT} rate constant is identical for the eight cases studied in this article.

The last column in Table III provides the primary kinetic isotope effect (KIE) for the reaction HO + DOD → HOD + OD. Because tunneling preferentially favors protium transfer more than deuterium transfer, it is clear that the deeper the well, the greater the KIE turns out to be. On the other hand, the Arrhenius parameters at different temperatures derived from the four curves depicted in Figure 3 are given in Table IV. Just the same trends discussed for Table II hold here, although now the variation of the tunneling contribution and the corresponding effects are entirely due to the change of the depth of the minimum.

Finally, it is interesting to compare the kinetic parameters calculated for the curve 4 in Figure 2 (no complex formation; see Tables I and II) with the ones obtained from the curve 1 in Figure 3 (original system including the formation of two complexes; see Tables III and IV). Despite the fact that the k^{CVT} rate constant is the same, the formation of the complexes in the original system influence the shape of the potential energy surface, increasing tunneling in such a way that its kinetic parameters differ crucially from the ones obtained in absence of the

TABLE IV.

Preexponential Factors (in cm^3 $Molecule^{-1}$ s^{-1}) and Activation Energies (in kcal/mol) at Several Temperatures (Power of 10 in Parentheses) for the Reactions Corresponding to the Four Curves Depicted in Figure 3.

	300 K		300–420 K		700 K	
Curve	A	E_a	A	E_a	A	E_a
1	9.44(−15)	3.73	2.62(−14)	4.34	4.73(−13)	7.27
2	3.04(−14)	5.02	5.90(−14)	5.41	5.66(−13)	7.74
3	4.01(−14)	5.32	7.14(−14)	5.67	5.89(−13)	7.85
4	4.78(−14)	5.54	8.12(−14)	5.85	6.11(−13)	7.94

minima (for instance, $k^{CVT/SCT}$ increases more than 1800 times at 300 K).

Concluding Remarks

It is clear that the one-step low-pressure rate constant of a bimolecular gas-phase reaction that takes place by classical thermal activation over a transition state that lies energetically quite above the reactants does not depend on the existence of any minimum potential energy (complex) along the minimum energy path below the reactants. However, we have shown in this article that the scenario changes dramatically if the reaction proceeds by tunneling. Because existence of a complex reduces the thickness of the classically forbidden region for the energies below the adiabatic barrier, tunneling is increased and the reaction is accelerated. As the well becomes deeper, the effect is greater. The kinetic magnitudes, such as the Arrhenius parameters and the kinetic isotope effect, turn out to be noticeably modified. In particular, the activation energies and the preexponential factors of these reactions are quite small, even at room temperature or higher.

An important warning stems from these results: a theoretical study of the kinetics of a low-pressure reaction that can proceed by tunneling must take into account any potential energy minimum that can appear along the minimum energy path preceding (or following) the transition state to be reliable. Many atmospheric reactions that initially proceed via a hydrogen-bonded complex formation can be considered to fall within the present description.

References

1. (a) Wayne, R. F. In: Chemistry of Atmospheres; Clarendon Press: Oxford, 1991, 2nd ed.; (b) Atkinson, R. In: Herter, R. E.; Harrison, R. M., eds. Issues in Environmental Science and Technology; The Royal Society of Chemistry: London, 1995, 4, p. 65.
2. (a) Dubey, M. K.; Mohrschladt, R.; Donahue, N. M.; Anderson, J. G. J Phys Chem A 1997, 101, 1494; (b) Sekušak, S.; Liedl, K. R.; Rode, B. M.; Sabljić, A. J Phys Chem A 1997, 101, 4245; (c) Masgrau, L.; González-Lafont, A.; Lluch, J. M. J Phys Chem A 1999, 103, 1044.
3. Frank, I.; Parrinello, M.; Klamt, A. J Phys Chem A 1998, 102, 3614.
4. (a) Truhlar, D. G.; Isaacson, A. D.; Garrett, B. C. In: Baer, M., ed. Theory of Chemical Reaction Dynamics; CRC Press: Boca Raton, FL, 1985, p. 65; (b) Hu, W.-P.; Truhlar, D. G. J Am Chem Soc 1995, 117, 10726; (c) Hu, W.-P.; Truhlar, D. G. J Am Chem Soc 1996, 118, 860.
5. Villà, J.; González-Lafont, A.; Lluch, J. M. J Phys Chem 1996, 100, 19389.
6. Villà, J.; Truhlar, D. G. Theoret Chem Acc 1997, 97, 317.
7. González-Lafont, A.; Truong, T. N.; Truhlar, D. G. J Chem Phys 1991, 12, 8875.
8. Hu, W.-P.; Liu, Y.-P.; Truhlar, D. G. J Chem Soc Faraday Trans 1994, 90, 1715.
9. (a) Garrett, B. C.; Truhlar, D. G. J Am Chem Soc 1979, 101, 4534; (b) Garrett, B. C.; Truhlar, D. G. J Am Chem Soc 1979, 101, 5207; (c) Tucker, S. C.; Truhlar, D. G. In: Bertrán, J.; Csizmadia, I. G., eds. New Theoretical Concepts for Understanding Organic Reactions; Kluwer Academic: Dordrecht, 1989, p. 291; (d) Truhlar, D. G.; Gordon, M. S. Science 1990, 249, 491.
10. (a) Lu, D.-h.; Truong, T. N.; Melissas, V. S.; Lynch, G. C.; Liu, Y.-P.; Garrett, B. C.; Steckler, R.; Isaacson, A. D.; Rai, S. N.; Hancock, G. C.; Lauderdale, J. G.; Joseph, T.; Truhlar, D. G. Comput Phys Commun 1992, 17, 235; (b) Liu, Y.-P.; Lynch, G. C.; Truong, T. N.; Lu, D.-h.; Truhlar, D. G.; Garrett, B. C. J Am Chem Soc 1993, 115, 2408.
11. Corchado, J. C.; Chuang, Y.-Y.; Fast, P. L.; Villà, J.; Coitiño, E. L.; Hu, W.-P.; Liu, Y.-P.; Lynch, G. C; Nguyen, K. A.; Jackels, C. F.; Gu, M. Z.; Rossi, I.; Clayton, S.; Melissas, V. S.; Steckler, R.; Garrett, B. C.; Isaacson, A. D.; Truhlar, D. G. POLYRATE, version 7.9.1; University of Minnesota, Minneapolis, 1998.